# Repulsive and attractive Casimir forces in a glide-symmetric geometry

Alejandro W. Rodriguez,[1] J. D. Joannopoulos,[1] and Steven G. Johnson[2]
[1]*Department of Physics, Massachusetts Institute of Technology, Cambridge, Massachusetts 02139, USA*
[2]*Department of Mathematics, Massachusetts Institute of Technology, Cambridge, Massachusetts 02139, USA*
(Received 31 January 2008; published 17 June 2008)

We describe a three-dimensional geometry in which both attractive and repulsive Casimir forces arise using ordinary metallic materials, as computed via an exact numerical method (no uncontrolled approximations). The geometry consists of a zipperlike, glide-symmetric structure formed of interleaved metal brackets attached to parallel plates—because of the interleaving pattern, a net repulsive force can arise from a combination of attractive interactions. Depending on the separation, the perpendicular force between the plates and brackets varies from attractive (large separations) to repulsive (intermediate distances) and back to attractive (close separations), with one point of stable equilibrium in the perpendicular direction. This geometry was motivated by a simple intuition of attractive interactions between surfaces, and so we also consider how a rough proximity-force approximation of pairwise attractions compares to the exact calculations.

DOI: 10.1103/PhysRevA.77.062107 PACS number(s): 12.20.Ds, 42.50.Lc, 42.82.−m, 85.85.+j

## I. INTRODUCTION

We describe a metallic, glide-symmetric, "Casimir zipper" structure (depicted in Fig. 1) in which both repulsive and attractive Casimir forces arise, including a point of stable equilibrium with respect to perpendicular displacements. Here, the forces are "repulsive" in the sense that they act to separate the two structures, but in some sense they are a combination of attractive interactions as discussed below. We compute the force using an "exact" computational method (i.e., with no uncontrolled approximations, so that it yields arbitrary accuracy given sufficient computational resources), and compare these results to the predictions of an *ad-hoc* attractive interaction based on the proximity-force approximation (PFA). Casimir forces, a result of quantum vacuum fluctuations, arise between uncharged objects, most typically as an attractive force between parallel metal plates [1] that has been confirmed experimentally [2,3]. One interesting question has been whether the Casimir force can manifest itself in ways very different from this monotonically decaying attractive force, and especially under what circumstances the force can become repulsive. It has been proven that the Casimir force is always attractive in a mirror-symmetric geometry of dielectric materials with $\varepsilon \geq 1$ on the imaginary-frequency axis [4], but there remains the possibility of repulsive forces in asymmetric structures and/or with different materials. For example, repulsive forces arise in exotic asymmetric material systems, such as a combination of magnetic and electric materials [5–7] (with some suggestions of metamaterials as route to realization [8–10]), fluid-separated dielectric plates [11], and possibly also in metamaterials with gain [8] or for excited atoms [12] (although this result of Ref. [8] is problematic because the Lifshitz formula may not be applicable to excited [12] or amplifying [10–13] media). Another route to unusual Casimir phenomena is to use conventional materials in complex geometries, which have been shown to enable asymmetrical lateral [14] or "ratchet" effects [15,16] and nonmonotonic dependencies on external parameters [17]. Both of the previous lateral effects [14,15] and the repulsive interaction described here intuitively arise from competing attractive contributions to the net force. The basic idea of using geometry to enable unusual Casimir phenomena provides an interesting supplement to the materials approach and could be useful in the design of experiments and technology involving the Casimir effect. Until recently, however, predictions of Casimir forces in geometries very different from parallel plates have been hampered by the lack of theoretical tools capable of describing arbitrary geometries, but this difficulty has been addressed (in principle) by recent numerical methods [18–21]. Here, we use a technique based on the mean Maxwell stress tensor computed numerically via an imaginary-frequency Green's function, which can handle arbitrary geometries and materials [18].

The geometry that we consider is depicted schematically in Fig. 1: We have two periodic sequences of metal "brackets" attached to parallel metal plates, which are brought into close proximity in an interlocking "zipper" fashion. In Fig. 1, we have colored the two plates and brackets red and blue to distinguish them, but they are made of the same metallic material. This structure is not mirror symmetric (and in fact

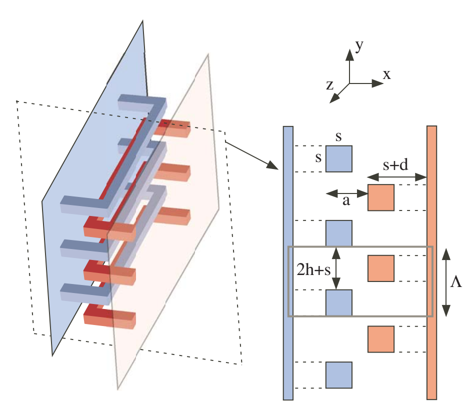


FIG. 1. (Color online) Three-dimensional schematic of the Casimir "zipper" geometry of interlocking metal brackets (shown in different colors for illustration only), along with a two-dimensional $xy$ cross section. The dashed lines extruding from the plates to the squares indicate their out-of-plane connectivity.

 

is glide symmetric, although the glide symmetry is not crucial), so it is not required to have an attractive Casimir force by Ref. [4]. Furthermore, the structure is connected and the objects can be separated via a rigid motion parallel to the force (a consideration that excludes interlocking "hooks" and other geometries that trivially give repulsive forces). This structure is best understood by considering its two-dimensional cross section, shown in Fig. 1 (right-hand side) for the middle of the brackets: In this cross section, each bracket appears as an $s \times s$ square whose connection to the adjacent plate occurs out-of-plane. (Here, the brackets are repeated in each plate with period $\Lambda = 2s + 2h$ and are separated from the plates by a distance $d$. The plates are separated by a distance $2d + s + a$, so that $a = 0$ is the point where the brackets are exactly aligned.) The motivation for this geometry is an intuitive picture of the Casimir force as an attractive interaction between surfaces. When the plates are far apart and the brackets are not interlocking, the force should be the ordinary attractive one. As the plates move closer together, the force is initially dominated by the attractions between adjacent bracket squares, and as these squares move past one another ($a < 0$ in Fig. 1), one might hope that their attraction leads to a net repulsive force pushing the plates apart. Finally, as the plates move even closer together, the force should be dominated by the interactions between the brackets and the opposite plate, causing the force to switch back to an attractive one. This intuition must be confirmed by an exact numerical calculation, however, because actual Casimir forces are not two-body attractions, are not generally additive, and can sometimes exhibit qualitatively different behaviors than a two-body model might predict [5,17,22,23]. Such a computation of the total force per unit area is shown in Fig. 2, and demonstrates precisely the expected sign changes in the force for the three separation regimes. These results are discussed in greater detail below.

Previous theoretical studies of Casimir forces in geometries with strong curvature have considered a variety of objects and shapes. Forces between isolated spheres [21] and isolated cylinders [24], or between a single sphere [25], or cylinder [20,25] and a metal plate, all exhibit attractive forces that decrease monotonically with separation. When a pair of squares [17] or cylinders [24] interacts in the presence of two adjacent metal sidewalls, the force is still attractive and monotonic in the square-square or cylinder-cylinder separation, but is a nonmonotonic function of the sidewall separation. When two corrugated surfaces are brought together in a way that breaks mirror symmetry (i.e., the corrugations are not aligned between the two surfaces), a lateral force can arise [26,27], and an asymmetric lateral force from asymmetric corrugations can lead to a "ratchet" effect in which random forces preferentially displace the plates in one direction [15]. Such a lateral force has also been observed experimentally [28]. In the geometry of Fig. 1, in contrast, there is no lateral force (due to a mirror-symmetry plane perpendicular to the plates), and hence we consider only the normal force between the plates. Because of the strong curvature of the surfaces relative to their separations, simple parallel-plate approximations are not valid (although we consider their qualitative accuracy below), and the force must be computed numerically.

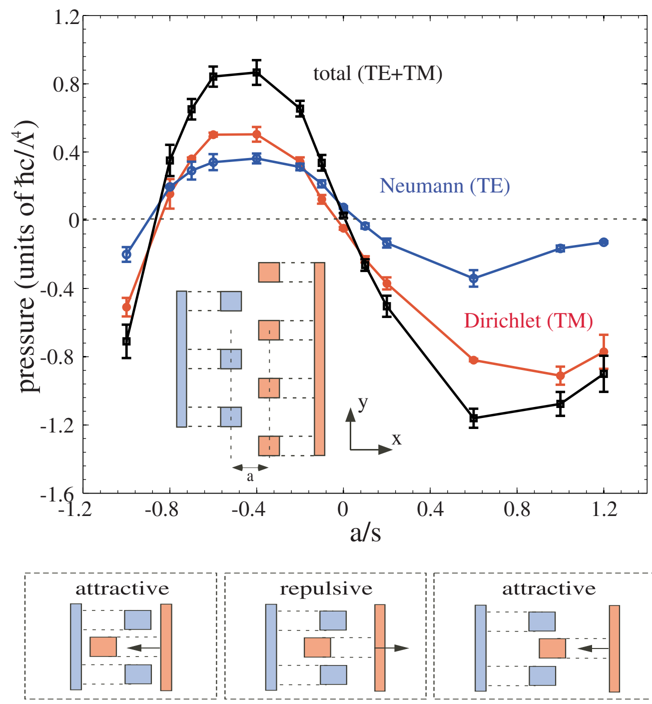


FIG. 2. (Color online) Top: Plot of the Neumann (blue, TE), Dirichlet (red, TM) and total (black, TE+TM) Casimir pressure (in units of $\hbar c/\Lambda^4$) between the objects of Fig. 1, as a function of $a/s$. The inset illustrates a two-dimensional cross section. Bottom: Schematic indicating the various qualitatively different Casimir force regimes between the two structures.

## II. NUMERICAL RESULTS

The numerical method we employ is based on integration of the mean stress tensor, evaluated in terms of the imaginary-frequency Green's function via the fluctuation-dissipation theorem [18]. The Green's function can be evaluated by a variety of techniques, but here we use a simple finite-difference frequency-domain method [18,29] that has the advantage of being very general and simple to implement at the expense of computational efficiency. In particular, the computation involves repeated evaluation of the electromagnetic Green's function, integrated over imaginary frequency $w = -i\omega$ and a surface around the object of interest. The Green's function is simply the inverse of a linear operator $[\nabla \times \nabla \times + w^2 \varepsilon(iw, \mathbf{r})]$, which here is discretized using a finite-difference Yee grid [29] and inverted using the conjugate-gradient method [30]. In order to simplify the calculations, we assume the length of the brackets in the $z$ direction $L$ to be sufficiently long to make their contributions to the force negligible (we estimate the minimum length below). We can therefore describe the geometry as both $z$ invariant and $y$ periodic (with period $\Lambda$). This implies that it is only necessary to compute the Green's function using an $xy$ unit cell, with the periodic and invariant directions handled by integrating over the corresponding wave vectors [18]. Furthermore, we approximate the bracket and plate materials by perfect metals, valid in the limit of small length scales (which are dominated by long-wavelength contributions where the skin depth is negligible). In this case, the contributions to the force can be separated into two polarizations: transverse electric (TE) with the electric field in the $xy$ plane (a scalar magnetic field with Neumann boundary conditions); and transverse magnetic (TM) with the magnetic field in the $xy$ plane (a scalar electric field with Dirichlet boundary conditions) [18], and these two contributions are shown separately in Fig. 2.

The resulting force per unit area between the plates, for the chosen parameters $d/s=2$ and $h/s=0.6$, is plotted as a function of $a/s$ in Fig. 2 (top); error bars show estimates of the numerical accuracy due to the finite spatial resolution. A number of unusual features are readily apparent in this plot. First, the sign of the force changes not only once, but twice. The corresponding zeros of the force lie at $a/s \approx -0.8$ and $a/s \approx -10^{-2}$. The first zero, $a/s \approx -0.8$, is a point of unstable equilibrium, to the left of which the force is attractive and to the right of which the force is repulsive. The second zero at $a/s \approx -10^{-2}$ corresponds to a point of stable equilibrium, with respect to perpendicular displacements, for which the force is attractive to the right and repulsive to the left. (This point is still unstable with respect to lateral displacements, parallel to the plates and perpendicular to the brackets, however: Any such lateral displacement will lead to a lateral force that pulls the red and blue brackets together.) In between these equilibria, the repulsive force has a local maximum at $a/s \approx -0.5$. Finally, at $a/s \approx 0.6$ the magnitude of the attractive force reaches a local maximum (a local minimum in the negative force on the plot), and then decreases asymptotically to zero as $a/s \to \infty$. Thus, as the two objects move apart from one another, the force between them varies in a strongly nonmonotonic fashion (distinct from the nonmonotonic dependence on an external parameter shown in our previous work [17,22,24]). These three different sign regimes are shown schematically in Fig. 2 (bottom), as predicted by the intuitive picture described above.

## III. COMPARISON TO PROXIMITY-FORCE APPROXIMATION

Since the qualitative features of the Casimir force in this geometry correspond to the prediction of an intuitive model of pairwise surface attractions, it is reasonable to ask how such a model compares quantitatively with the numerical results. The most common such model is the proximity-force approximation (PFA), which treats the force as a summation of simple "parallel-plate" contributions [25]. (Another pairwise power-law heuristic is the "Casimir-Polder interaction" approximation, strictly valid only in the limit of dilute media [31].) Applied to a geometry with strong curvature and/or sharp corners such as this one, PFA is an uncontrolled approximation and its application is necessarily somewhat *ad-hoc* (due to an arbitrary choice of which points on the surfaces to treat as "parallel plates"), but it remains a popular way to quantify the crude intuition of Casimir forces as pairwise attractions.

Applying the PFA approximation to the two objects in Fig. 1, we treat the net force as a sum of three contributions: The force between the two parallel plates, the force between each square and the opposite plate, and the force between adjacent red and blue squares. Namely,

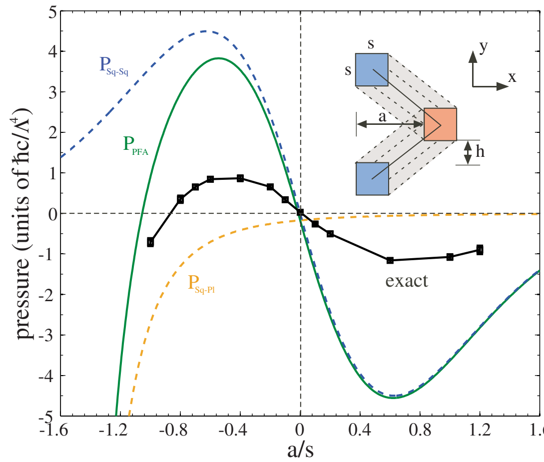


FIG. 3. (Color online) Comparison of Casimir pressure (in units of $\hbar c/\Lambda^4$) as a function of $a/s$ between the stress-tensor (exact) numerical results (black squares) and the proximity-force approximation (solid green). Also shown are the individual square-square (dashed blue) and square-plate (dashed orange) contributions to the PFA force. Inset: Schematic illustration of the chosen PFA "lines of interaction" between squares (dashed black lines).

$$P_{\text{PFA}} = \frac{1}{\Lambda L}(F_{\text{pl-pl}} + 2F_{\text{sq-pl}} + 2F_{\text{sq-sq}}), \tag{1}$$

where the first term is the pressure between two parallel plates (pl-pl), and the two remaining terms correspond to the square-plate (sq-pl) and square-square (sq-sq) interactions. The factors of $\Lambda$ and $L$ are introduced because these expressions are computed per unit length in the $z$ direction, and per period in the $y$ direction.

The first two PFA contributions are relatively simple to calculate because they are between parallel metal surfaces, and thus (in the PFA approximation) are the ordinary Casimir force weighted by the respective areas,

$$P_{\text{pl-pl}} = -\frac{\hbar c \pi^2 h}{120\Lambda}\frac{1}{(2d+a+s)^4} \tag{2}$$

$$P_{\text{sq-pl}} = -\frac{\hbar c \pi^2 s}{240\Lambda}\frac{1}{(d+a)^4} \tag{3}$$

Computing the square-square force is less straightforward, since there is some ambiguity as to what the PFA approximation even means for two nonparallel surfaces (separate from the question of its accuracy). In PFA, one adds up "parallel plate" contributions to the force between two objects by including a force between each point on one surface and a corresponding point on the other surface, where corresponding points are connected by parallel "lines of interaction." In this geometry, we take the lines of interaction to lie parallel to the center-to-center displacement between two squares, as depicted by the inset in Fig. 3, but of course this choice is somewhat arbitrary. (A similar choice was made in Ref. [32] to define the PFA force between two eccentric cylinders.) The PFA force between one pair of squares is then

$$P_{\text{sq-sq}} = -\frac{\hbar c \pi^2 a}{240\Lambda D^5}\left\{\left[\frac{2|a|}{3}(H^3-1)+\frac{sH^3}{h}(Hh-|a|)\right]\times\Theta(Hh-a)+\left[\frac{2Hh}{3}(A^3-1)+\frac{sA^3}{|a|-s}(|a|-Hh)\right]\times\Theta(|a|-Hh)\right\}, \tag{4}$$

where $D\equiv\sqrt{a^2+(h+s)^2}$, $H\equiv 1+s/h$, and $A\equiv 1-s/|a|$. The resulting net force is shown in Fig. 3, along with the contributions due to the isolated square-square and square-plate PFA forces (a separate line for the plate-plate contributions is not shown because this contribution is always very small).

For comparison, Fig. 3 also shows the exact total force from Fig. 2, and it is clear that, while PFA captures the qualitative behavior of the oscillating force sign, in quantitative terms it greatly overestimates the magnitude of the repulsive force. Of course, since it is an uncontrolled approximation in this regime there is no reason to expect quantitative accuracy, but the magnitude of the error illustrates how different the true Casimir force is from this simple estimate. The PFA estimate for the square-plate force, however, does help us to understand one feature of the exact result. If there were no plates, only squares, then the force would be zero by symmetry exactly at $a=0$, and indeed the exact result including the plates has zero force at $a\approx 0$; clearly, the contribution to the force from the plates is negligible for $a\approx 0$, and this is echoed by the PFA $P_{\text{sq-pl}}$ force. Also, using a PFA approximation, one can attempt to estimate the order of magnitude of the force contribution from the ends of the bracket, which was neglected in the exact calculation. This contribution to the total force must decrease as $\sim 1/L$ for a fixed $a$, and is estimated to be less than 1% of the peak repulsive force for $L\gtrsim 60\Lambda$.

## IV. CONCLUDING REMARKS

Because the basic explanation for the sign changes in the force for this structure is fundamentally geometrical, we expect that the qualitative behavior will be robust in the face of imperfect metals, surface roughness, and similar deviations from the ideal model here. The main challenge for an experimental realization (for example, to obtain a mechanical oscillator around the equilibrium point) would appear to be maintaining a close parallel separation of the brackets (although it may help that in at least one direction this parallelism is a stable equilibrium). Furthermore, although in this paper we demonstrated one realization of a geometry-based repulsive Casimir force, this opens the possibility that future work will reveal similar phenomena in many other geometries, perhaps ones more amenable to experiment.

Since the repulsion between the two objects here appears to be a result of attractive interactions between surfaces, our result also invites the following unanswered question: Is it possible to design a geometry with a repulsive Casimir interaction, with ordinary vacuum-separated metallic materials, that cannot be understood as a combination of surface attractions? More precisely, can one obtain a repulsive Casimir interaction between a metallic or dielectric object lying in $x<0$ and another lying in $x>0$, i.e., two objects with a separating plane in vacuum, so that the distances between the surfaces are strictly nondecreasing as they are moved apart? The geometry here does not have a separating plane in the repulsive regime, while Ref. [4] only eliminated the mirror-symmetric case, so either a more general theorem or an asymmetric counterexample would represent important developments.


## ACKNOWLEDGMENTS

This work was supported in part by U.S. Department of Energy Grant No. DE-FG02-97ER25308 and by MRSEC NSF program Grant No. DMR-0213282. We are also grateful to M. Ibanescu and D. Dalvit for useful discussions.



[1] H. B. G. Casimir, Proc. K. Ned. Akad. Wet. **51**, 793 (1948).
[2] S. K. Lamoreaux, Phys. Rev. Lett. **78**, 5 (1997).
[3] U. Mohideen and A. Roy, Phys. Rev. Lett. **81**, 4549 (1998).
[4] O. Kenneth and I. Klich, Phys. Rev. Lett. **97**, 160401 (2006).
[5] O. Kenneth, I. Klich, A. Mann, and M. Revzen, Phys. Rev. Lett. **89**, 033001 (2002).
[6] C.-G. Shao, D.-L. Zheng, and J. Luo, Phys. Rev. A **74**, 012103 (2006).
[7] T. H. Boyer, Phys. Rev. A **9**, 2078 (1974).
[8] U. Leonhardt and T. G. Philbin, New J. Phys. **9**, 254 (2007).
[9] C. Henkel and K. Joulain, Europhys. Lett. **72**, 929 (2005).
[10] F. S. S. Rosa, D. A. R. Dalvit, and P. W. Milonni, Phys. Rev. Lett. **100**, 183602 (2008).
[11] J. N. Munday and F. Capasso, Phys. Rev. A **75**, 060102(R) (2007).
[12] Y. Sherkunov, Phys. Rev. A **72**, 052703 (2005).
[13] C. Raabe and D.-G. Welsch, e-print arXiv:0710.2867.
[14] T. Emig, A. Hanke, R. Golestanian, and M. Kardar, Phys. Rev. Lett. **87**, 260402 (2001).
[15] T. Emig, Phys. Rev. Lett. **98**, 160801 (2007).
[16] M. Miri and R. Golestanian, Appl. Phys. Lett. **92**, 113103 (2008).
[17] A. Rodriguez, M. Ibanescu, D. Iannuzzi, F. Capasso, J. D. Joannopoulos, and S. G. Johnson, Phys. Rev. Lett. **99**, 080401 (2007).
[18] A. Rodriguez, M. Ibanescu, D. Iannuzzi, J. D. Joannopoulos, and S. G. Johnson, Phys. Rev. A **76**, 032106 (2007).
[19] H. Gies, K. Langfeld, and L. Moyaerts, J. High Energy Phys. (2003) 18.
[20] T. Emig, R. L. Jaffe, M. Kardar, and A. Scardicchio, Phys. Rev. Lett. **96**, 080403 (2006).
[21] T. Emig, N. Graham, R. L. Jaffe, and M. Kardar, Phys. Rev. Lett. **99**, 170403 (2007).
[22] S. Zaheer, A. W. Rodriguez, S. G. Johnson, and R. L. Jaffe, Phys. Rev. A **76**, 063816 (2007).
[23] H. Gies and K. Klingmuller, Phys. Rev. Lett. **96**, 220401

(2006).
[24] S. J. Rahi, A. W. Rodriguez, T. Emig, R. L. Jaffe, S. G. Johnson, and M. Kardar, Phys. Rev. A **77**, 030101(R) (2008).
[25] M. Bordag, Phys. Rev. D **73**, 125018 (2006).
[26] T. Emig, A. Hanke, R. Golestanian, and M. Kardar, Phys. Rev. A **67**, 022114 (2003).
[27] R. B. Rodrigues, P. A. Maia Neto, A. Lambrecht, and S. Reynaud, Europhys. Lett. **76**, 822 (2006).
[28] F. Chen, U. Mohideen, G. L. Klimchitskaya, and V. M. Mostepanenko, Phys. Rev. Lett. **88**, 101801 (2002).
[29] A. Christ and H. L. Hartnagel, IEEE Trans. Microwave Theory Tech. **35**, 688 (1987).
[30] Z. Bai, J. Demmel, J. Dongarra, A. Ruhe, and H. Van Der Vorst, *Templates for the Solution of Algebraic Eigenvalue Problems: A Practical Guide* (SIAM, Philadelphia, 2000).
[31] M. Tajmar, Int. J. Mod. Phys. C **15**, 1387 (2004).
[32] D. A. R. Dalvit, F. C. Lombardo, F. D. Mazzitelli, and R. Onofrio, Europhys. Lett. **67**, 517 (2004).